Hindawi Publishing Corporation
International Journal of Photoenergy
Volume 2013, Article ID 843615, 9 pages
http://dx.doi.org/10.1155/2013/843615

Research Article

Solution-Processed Bulk Heterojunction Solar Cells with Silyl End-Capped Sexithiophene

Jung Hei Choi,[1] Mohamed E. El-Khouly,[2] Taehee Kim,[1] Youn-Su Kim,[1] Ung Chan Yoon,[3] Shunichi Fukuzumi,[4] and Kyungkon Kim[1,5]

[1] *Photo-Electronic Hybrids Research Center, Korea Institute of Science and Technology, Hwarangno 14-gil 5, Seongbuk-gu, Seoul 136-791, Republic of Korea*
[2] *Department of Chemistry, Faculty of Science, Kafrelsheikh University, Kafr ElSheikh 33516, Egypt*
[3] *Department of Chemistry, Pusan National University, Jangjeon-dong Kumjeong-gu, Busan 609-735, Republic of Korea*
[4] *Department of Material and Life Science, Graduate School of Engineering, Osaka University, ALCA, Japan Science and Technology Agency (JST), Suita, Osaka 565-0871, Japan*
[5] *Department of Chemistry and Nanoscience, Ewha Womans University, 52 Ewhayeodae-gil, Seodaemun-gu, Seoul 120-750, Republic of Korea*

Correspondence should be addressed to Shunichi Fukuzumi; fukuzumi@chem.eng.osaka-u.ac.jp

Received 15 July 2013; Accepted 25 November 2013

Academic Editor: Adel M. Sharaf

Copyright © 2013 Jung Hei Choi et al. This is an open access article distributed under the Creative Commons Attribution License, which permits unrestricted use, distribution, and reproduction in any medium, provided the original work is properly cited.

We fabricated solution-processed organic photovoltaic cells (OPVs) using substituted two sexithiophenes, a,w-bis(dimethyl-*n*-octylsilyl)sexithiophene (**DSi-6T**) and a,w-dihexylsexithiophene (**DH-6T**), as electron donors, and [6,6]-phenyl-C_{61}-butyric acid methyl ester (PCBM) as an electron acceptor. Solution-processed OPVs using **DH-6T** and **DSi-6T** showed good photovoltaic properties in spite of their poor solubility. The best performance was observed on **DSi-6T** : PCBM 1 : 5 (w/w) blend cell with an open circuit voltage (V_{oc}) of 0.63 V, short circuit current density (J_{sc}) of 1.34 mA/cm^2, fill factor (FF) of 55%, and power conversion efficiency of 0.44% under AM 1.5 G illumination. Although **DH-6T** has higher hole mobility than **DSi-6T**, the **DSi-6T** : PCBM blend cell showed higher hole mobility than **DH-6T** : PCBM cell. Therefore, **DSi-6T** cell showed higher device performance than **DH-6T** cell due to its silyl substitutions, which lead to the increase of the solubility. The incorporation of solution-processed TiO_2 interfacial layer in the **DSi-6T** : PCBM devices significantly enhances FF due to the reduced charge recombination near active layer/Al interface.

1. Introduction

Organic solar cells have received strong attention due to the possibility to realize flexible and low-cost large photovoltaic cells [1–5]. Polymer based organic photovoltaic cells (OPVs) demonstrated power conversion efficiencies (PCEs) in excess of 7% by the results of synthesis of low bandgap polymers [6, 7]. However, the polymers still have high batch-to-batch variations and difficulty in purification, and there have been many efforts to discover solution-processed small molecules. Recently, oligothiophenes have received much attention as donor materials in OPVs because of their high hole mobility, easy multigram synthesis, high purity, and simple chemical modification [8–10]. Some studies on oligothiophene based solar cells have already been reported using bilayer heterojunction solar cells [11–15]. By controlling the film morphology using coevaporation of excess fullerene (C_{60}), bulk heterojunction organic photovoltaic cells consisting of sexithiophene (6T) as a donor and C_{60} as an acceptor showed good photovoltaic properties [16]. However, the small molecules based on sexithiophene have not been investigated solution-processed OPVs. The low performance of sexithiophene-based solar cells was mainly attributed to the difficulties encountered in fabricating solution-processed bulk heterojunction cells.

We choose α,ω-dihexylsexithiophene (**DH-6T**) as the oligothiophene material because it is well known to exhibit

high field-effect mobility as high as 1.0 cm^2/Vs and a representative oligothiophene material [17]. Recently, we reported α,ω-bis(dimethyl-*n*-octylsilyl)sexithiophene (**DSi-6T**) for vacuum-deposited or solution processable organic thin film transistor application [18]. The silyl end-capped sexithiophene (**DSi-6T**, 2.2 g/L in $CHCl_3$) was more soluble than hexyl substituted sexithiophene (**DH-6T**, 1 g/L in $CHCl_3$) [19]. Thus, the silyl end-capped sexithiophene may be a good candidate for solution processable solar cell application.

In regard to our continuing interest for sexithiophene-based organic solar cells, we report herein analysis of the performance of solution-processed organic solar cells based on α,ω-functionalized linear sexithiophene: PCBM systems. We fabricated the solution-processed OPVs using two linear sexithiophenes, α,ω-dihexylsexithiophene (**DH-6T**) and α,ω-bis(dimethyl-*n*-octylsilyl)sexithiophene (**DSi-6T**) as donors and [6, 6]-phenyl-C_{61}-butyric acid methyl ester (PCBM) as an acceptor (Figure 1). Solution-processed bulk heterojunction (BHJ) solar cells using **DH-6T** and **DSi-6T** with PCBM showed good photovoltaic properties in spite of their poor solubility. Although **DH-6T** has higher hole mobility than **DSi-6T**, the **DSi-6T** : PCBM blend cell showed higher hole mobility than **DH-6T** : PCBM cell. Therefore, **DSi-6T** cell showed higher device performance than **DH-6T** cell due to their silyl substitutions, which lead to the increase of the solubility. The higher photovoltaic performance of **DSi-6T** cell can be explained by the film morphology dependence on the solubility of donor. In addition, utilizing the nanosecond transient absorption spectroscopy in polar media in the visible and near-IR region proved electron-transfer reactions in DH-6T : PCBM and DSi-6T : PCBM mixtures.

2. Experimental Section

2.1. Instruments. The absorption spectra were measured using a Perkin Elmer Lambda 35 UV-vis spectrometer in spin-coated films at room temperature. The morphology of the **DSi-6T** : PCBM and **DH6T** : PCBM was determined using atomic force microscopy (AFM) (Park systems) operating in a noncontact mode, under ambient conditions. Steady-state fluorescence measurements were carried out on a Shimadzu spectrofluorophotometer (RF-5300PC). Phosphorescence spectra were obtained by a SPEX Fluorolog τ_3 spectrophotometer. Emission spectra in the visible region were detected by using a Hamamatsu Photonics R5509-72 photomultiplier. A deaerated 2-MeTHF solution containing **DH-6T** and **DSi-6T** at 77 K was excited at indicated wavelengths. Cyclic voltammograms (CV) and differential pulse voltammograms (DPV) techniques were carried on a BAS CV 50 W Voltammetric Analyzer. A platinum disk electrode was used as working electrode, while a platinum wire served as a counter electrode. SCE electrode was used as a reference electrode. All measurements were carried out in deaerated benzonitrile containing tetra-*n*-butylammonium hexafluorophosphate ($TBAPF_6$; 0.10 M) as a supporting electrolyte. The scan rate = 50 mV/s.

DSi-6T and **DH-6T** were excited by a Panther OPO pumped by Nd:YAG laser (Continuum, SLII-10, 4–6 ns fwhm) at λ = 440 nm with the powers of 1.5 and 3.0 mJ *per* pulse. The transient absorption measurements were performed using a continuous xenon lamp (150 W) and an InGaAs-PIN photodiode (Hamamatsu 2949) as a probe light and a detector, respectively. The output from the photodiodes and a photomultiplier tube was recorded with a digitizing oscilloscope (Tektronix, TDS3032, 300 MHz). All measurements were conducted at 298 K. The transient spectra were recorded using fresh solutions in each laser excitation.

2.2. Fabrication of BHJ Cells. BHJ solar cells were fabricated on patterned ITO (indium tin oxide) coated glass substrates as the anode. ITO on glass substrates was sequentially cleaned with isopropyl alcohol, acetone, and isopropyl alcohol in ultrasonic baths. Afterwards, it was dried in oven at 80°C for 10 min and then treated with UV-ozone for 20 min. The surface of the ITO substrate was modified by spin-coating conducting poly(3,4-ethylenedioxythiophene) : poly(styrenesulfonate) (PEDOT : PSS, H. C. Starck Baytron P VP Al 4083) with a thickness of around 40 nm, followed by baking at 120°C for 10 min in oven. The molecular structures of the donor (**DSi-6T** and **DH-6T**) and acceptor materials (PCBM) and their energy band diagram are shown in Figure 1. **DSi-6T** was synthesized according to literature procedures [18]. **DH-6T** was purchased from Aldrich Chemical Co. and was used without further purification. **DSi-6T** : PCBM (1 : 4, 1 : 5, 1 : 6 w/w) and **DH-6T** : PCBM (1 : 4, 1 : 6 w/w) were blended together and dissolved in chloroform at a total concentration of 20 mg mL^{-1}. And then **DSi-6T** : PCBM blended solution was no filtration, but **DH-6T** : PCBM solution was filtered out through a 0.45 μm filter. The active layer was spin-cast at 4000 rpm from the solution of **DSi-6T** or **DH-6T** and PCBM (Nano-C) in chloroform. The thickness of the active layers was around 80 nm, as measured with an Alpha-step IQ. A solution containing 0.5 wt% TiO_2 nanoparticles in ethanol was spin-coat at a rate of 4000 rpm on top of the active layer. The synthesis of TiO_2 nanoparticles is described elsewhere [20, 21]. The cathode consists of 100 nm of aluminum and was thermally evaporated on top of the film through the use of a shadow mask to define an active area of 0.12 cm^2 under a base pressure of 1×10^{-6} Torr (1 Torr = 133.32 Pa). The devices were annealed at 60°C for 10 min in the thermal evaporator. The current density-voltage curves were obtained using a Keithley 2400 source-measure unit. The photocurrent was measured under illumination using a Newport class-A 100 mW cm^{-2} solar simulator (AM 1.5 G) and the light intensity was calibrated with an NREL-calibrated Si solar cell with KG-1 filter for approximating one sun light intensity. External quantum efficiency (EQE) was measured in range from 300 to 800 nm using a specially designed EQE system (PV Measurements, Inc.). A 75 W xenon lamp was used as a light source for the generating monochromatic beam. A calibration was performed using a silicon photodiode, which was calibrated using the NIST-calibrated photodiode G425 as a standard, and IPCE values were collected under bias light at a low chopping speed of 10 Hz.

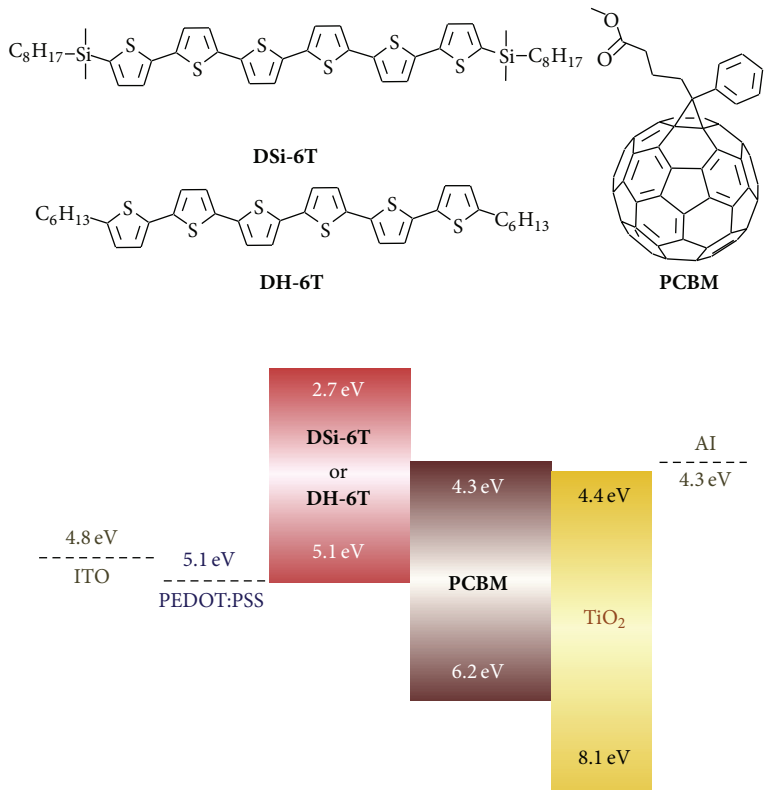

Figure 1: Chemical structures and energy band diagram of **DSi-6T**, **DH-6T**, and **PCBM**.

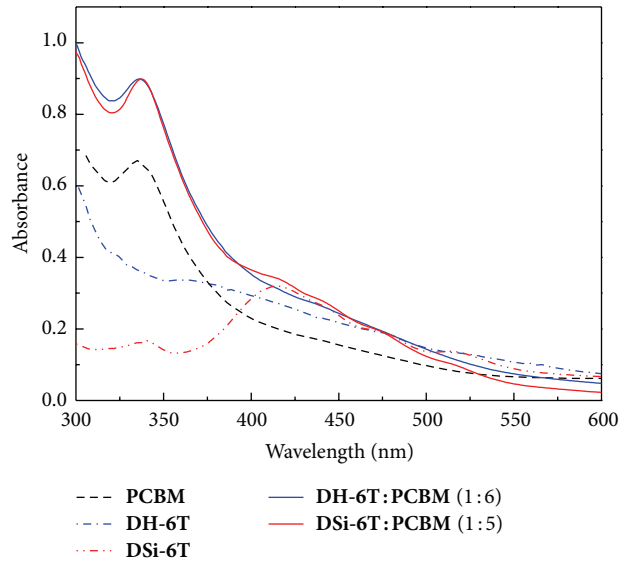

Figure 2: UV-vis absorption spectra of the **DSi-6T : PCBM** (1 : 5 w/w) and **DH-6T : PCBM** (1 : 6 w/w) blend films.

3. Results and Discussion

3.1. Electron-Transfer Reaction of DSi-6T/PCBM and DH-6T/PCBM. The UV-vis absorption spectra of spin-coated films of **DSi-6T** and **DH-6T** blended with PCBM are shown in Figure 2. Both **DH-6T** and **DSi-6T** exhibited similar absorption spectra in a dilute chloroform solution, with absorption maxima observed at 440 nm and 442 nm, respectively. The absorption spectra of sexithiophene films exhibited a noteworthy blue shift with respect to that in solution for both compounds, but this shift is more significant for **DH-6T** than for **DSi-6T**. While the **DH-6T** film showed the strongly blue-shifted absorption spectrum with maxima at 362 nm, the **DSi-6T** film showed an absorption peak at 415 nm. Such feature is attributed to molecular excitons formed as a consequence of the intermolecular interactions in the solid state [22] and is found to be blue-shifted by about 0.6 eV with respect to the characteristic absorption peaks of the isolated molecules. The PCBM film has an absorption band of about 340 nm and significantly greater absorption in the visible region (350–750 nm) compared to the PCBM solution, consistent with the literature [23]. The UV-vis absorption spectra of **DSi-6T : PCBM** (1 : 5 w/w) and **DH-6T : PCBM** (1 : 6 w/w) blend films showed similar shape due to their same backbone of donor and strong absorption of PCBM.

Fluorescence spectra of the singlet-excited state of **DH-6T** and **DSi-6T** in benzonitrile exhibited emission bands at 514 and 520 nm, respectively, from which the energy of the singlet state of **DH-6T** and **DSi-6T** were estimated as 2.41 and 2.39 eV, respectively (See Supporting Information, Figure S1 of Supplementary Material available online at http://dx.doi.org/10.1155/2013/843615). Fluorescence quantum yields of **DH-6T** and **DSi-6T** was determined as 0.13 and 0.36, respectively. Fluorescence lifetimes of the singlet states of **DH-6T** and **DSi-6T** were determined as 1.0 and

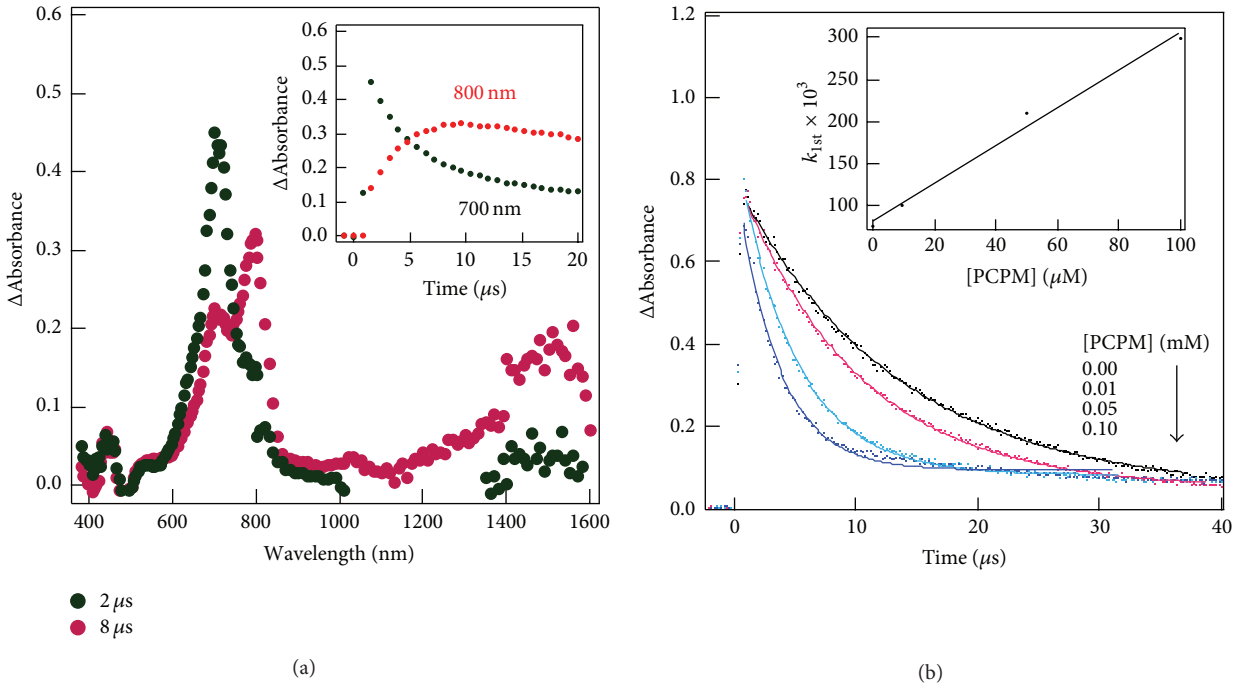

Figure 3: (a) Nanosecond transient spectra of **DSi-6T** (0.05 mM) in the presence of PCBM (0.05 mM) in deaerated benzonitrile; λ_{ex} = 440 nm. Inset: Decay time profile of ^{3}**DSi-6T*** (700 nm) and rise and decay profiles of **DSi-6T**$^{\bullet+}$(800 nm). (b) Dependence of rate constant of the formation of **DSi-6T**$^{\bullet+}$ at 800 nm on concentration of PCBM in deaerated benzonitrile. Inset: first-order plot.

1.8 ns, respectively. In the case of the DH-6T/PCBM and DSi-6T/PCBM mixtures, it was found that the fluorescence intensities and the lifetimes are quite close to those of the DH-6T and DSi-6T, respectively. This observation suggests the intermolecular electron transfer between the **DH-6T** and **DSi-6T** with PCBM, but not the intramolecular electron transfer.

The redox potentials of the examined **DH-6T**, **DSi-6T** and PCBM have been examined by using cyclic voltammetry (CV) and differential pulse voltammetry (DPV) techniques to evaluate the driving forces for the electron transfer ($-\Delta G_{et}{}^T$). The first reduction potential (E_{red}) of the PCBM was located at –856 mV versus Ag/$AgNO_3$, while the oxidation potentials (E_{ox}) of **DH-6T** and **DSi-6T** were located at 732 and 600 mV versus Ag/$AgNO_3$ (see Supporting Information, Figure S2–S5). The redox potential measurements of the **DH-6T**/PCBM and **DSi-6T**/PCBM mixtures did not show significant interaction suggesting no interaction in the ground state. The redox potentials of the examined **DH-6T**, **DSi-6T**, and PCBM suggest their potentials as promising materials in the photovoltaic cells. The feasibility of the electron-transfer process via the triplet-excited states is controlled by the free energy change ($\Delta G_{et}{}^T$), which can be expressed by the Rehm-Weller relation [24] (1):

$$\Delta G_{et}{}^T = E_{ox} - E_{red} - E_T + E_c, \quad (1)$$

where E_{ox} is the first oxidation potential of the **DH-6T** and **DSi-6T**, E_{red} is the first reduction potential of PCBM, E_T is the triplet energy of **DH-6T** (1.78 eV) and **DSi-6T** (1.79 eV) (we found from phosphorescence measurements in deaerated benzonitrile that energy level of the triplet **DH-6T** and **DSi-6T** at 1.78 and 1.79 eV, resp.), and E_c is the Coulomb energy term (approximately 0.06 eV in the polar benzonitrile) [25]. The free energy change ($\Delta G_{et}{}^T$) values *via* the triplet **DH-6T** and **DSi-6T** were estimated as −0.05 and −0.17 eV, respectively. The negative $\Delta G_{et}{}^T$ values suggest that the quenching process should be close to the diffusion-controlled limit (k_{diff}) [26].

By photoexcitation of **DSi-6T** in deaerated benzonitrile using 440 nm laser photolysis, the transient absorption spectrum immediately after the laser pulse exhibited only an absorption band at 700 nm, which assigned to the triplet-excited state of **DH-6T** (^{3}**DH-6T***) (See Supporting Information; Figure S6). By fitting the decay profile of ^{3}**DSi-6T***, the decay rate constant was found to be 6.60 × 10^4 s^{-1}, from which the lifetime of ^{3}**DSi-6T*** was estimated as 15.2 μs. By photoexcitation of **DSi-6T** in the presence of PCBM [0.01–0.10 mM] in Ar-saturated benzonitrile using 440 nm laser photolysis, the transient spectra exhibit the characteristic band of ^{3}**DSi-6T*** at 700 nm. With its decay, the concomitant rises of the **DSi-6T** radical cation (**DSi-6T**$^{\bullet+}$) at 800 and 1500 nm and the PCBM radical anion (PCBM$^{\bullet-}$) at 1000 nm were observed (Figure 3(a) and Figure S7). These observations show clear evidence of occurrence of intermolecular electron transfer from the triplet-excited state of **DSi-6T** to PCBM. In oxygen-saturated solutions, an intermolecular energy transfer from ^{3}**DSi-6T*** to oxygen emerges, suppressing the electron-transfer process. Similar

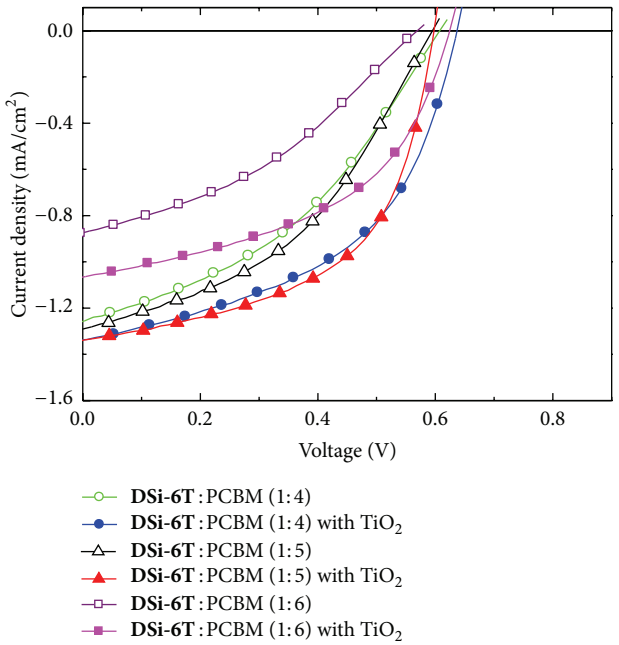

FIGURE 4: *J-V* characteristics of ITO/PEDOT : PSS/DSi-6T : PCBM/Al (active layer DSi-6T : PCBM 1 : 4, w/w (○), 1 : 5 w/w (△), 1 : 6 w/w (□)) and ITO/PEDOT : PSS/DSi-6T : PCBM/TiO_2/Al (active layer DSi-6T : PCBM 1 : 4, w/w (•), 1 : 5 w/w (▲), 1 : 6 w/w (■)) under illumination of AM 1.5, 100 mW cm^{-2}.

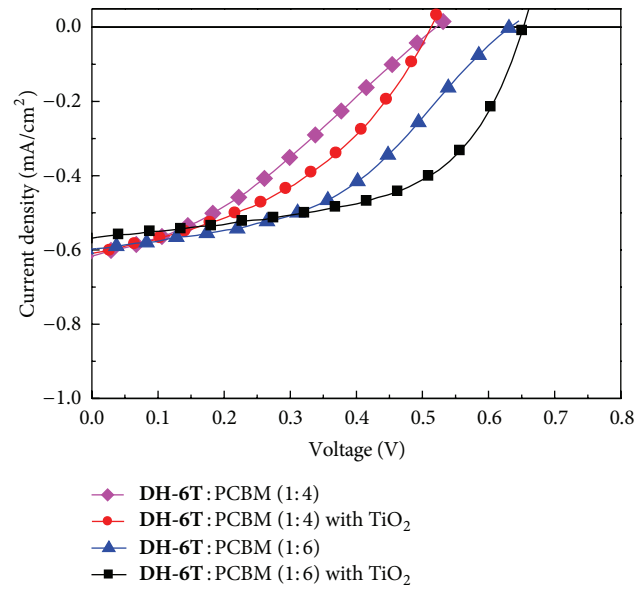

FIGURE 5: *J-V* characteristics of ITO/PEDOT : PSS/DH-6T : PCBM/Al (active layer DH-6T : PCBM 1 : 4, w/w (◆), 1 : 6 w/w (▲)) and ITO/PEDOT : PSS/DH-6T : PCBM/TiO_2/Al (active layer DH-6T : PCBM 1 : 4, w/w (•), 1 : 6 w/w (■)) under illumination of AM 1.5, 100 mW cm^{-2}.

electron-transfer features were recorded in the case of **DH-6T**/PCBM mixture in deaerated benzonitrile (See supporting information, Figure S8).

A more detailed picture of the kinetic is shown in Figure 3(b), where the rate constant of the electron-transfer process (k_{et}) was evaluated by monitoring the formation of the **DSi-6T**$^{\bullet+}$ as function of the concentrations of PCBM. The formation of **DSi-6T**$^{\bullet+}$ was fitted with clean first-order kinetics; each rate constant is referred to (k_{1st}). The linear concentration dependence of the observed k_{1st} values gives the k_{et}, which is calculated as 2.24×10^9 M^{-1} s^{-1}, which is near the diffusion-controlled limit ($k_{diff} = 5.6 \times 10^9$ M^{-1} s^{-1}) in benzonitrile [27]. Similarly, the k_{et} value of ^{3}**DH-6T***/PCBM mixture was found to be 2.65×10^9 M^{-1} s^{-1}, which is slightly larger than that of ^{3}**DSi-6T***/PCBM mixture (See supporting information, Figure S9).

3.2. Photovoltaic Properties of DSi-6T/PCBM and DH-6T/PCBM. For investigating the photovoltaic properties of sexithiophenes, OPVs were fabricated with the configuration of ITO/PEDOT : PSS/Donor (**DSi-6T** or **DH-6T**) : PCBM/Al. **DSi-6T** : PCBM and **DH-6T** : PCBM were blended together and dissolved in chloroform at a total concentration of 20 mg/mL. After Al deposition, the devices were thermally annealed at 60°C for 10 min. Figures 4 and 5 show the current density-voltage (*J-V*) curves of the OPV devices with **DSi-6T** : PCBM and **DH-6T** : PCBM using different blended ratios under AM 1.5 illumination, 100 mW cm^{-2}. Table 1 summarizes the photovoltaic performance of the functionalized sexithiophene based solar cells. The sexithiophene **DSi-6T** was mixed with PCBM to form bulk heterojunction active layers, for use as a donor with PCBM as an acceptor. The weight ratios of the donor to acceptor were 1 : 4, 1 : 5, and 1 : 6. For comparison, the OPV devices based on **DH-6T** : PCBM were also fabricated with commercial **DH-6T** as a donor and the weight ratio of 1 : 4 and 1 : 6. The short circuit current density (J_{sc}) values of the **DSi-6T** : PCBM BHJ solar cells increase as the weight ratio of donor to acceptor increases. However, the weight ratio of donor to accepter could not be larger than 1 : 4, due to low solubility of sexithiophenes. The photovoltaic performance was observed on **DSi-6T** : PCBM 1 : 5 (w/w) blend cell with an open circuit voltage (V_{oc}) of 0.60 V, a J_{sc} of 1.29 mA/cm^2, a fill factor (FF) of 42%, and power conversion efficiency of 0.32%. Under the same conditions, **DH-6T** : PCBM 1 : 6 (w/w) blend cell showed a V_{oc} of 0.63 V, a J_{sc} of 0.60 mA/cm^2, a FF of 44%, and PCE of 0.17%. The J_{sc} values of the **DH-6T** : PCBM cells were constant with 0.60 mA/cm^2 regardless of the weight ratio of **DH-6T** to acceptor. This result could be ascribed to the saturated solution of **DH-6T** : PCBM (1 : 6 w/w). In fact, a factor strongly affecting the J_{sc} of **DSi-6T** : PCBM cells is the filtration of the active solution. The J_{sc} of solar cell with the filtration of **DSi-6T** : PCBM solutions is 20% lower than that of solar cell without filtration. The most **DSi-6T** donors remained in the filter due to their strong π-π interaction. However, the **DH-6T** cells without filtration of active solutions showed the poor photovoltaic performance.

For the development of OPVs with increased PCE and lifetime, OPVs with the TiO_2 interfacial layer between the active layer and the Al electrode were fabricated together with typical OPVs without TiO_2. According to the literature,

Table 1: Photovoltaic characteristics of **DSi-6T** : PCBM and **DH-6T** : PCBM blended cells.

Device name	V_{oc} (V)	J_{sc} (mA/cm^2)	FF	PCE (%)
DSi-6T : PCBM				
1 : 4	0.61	1.26	0.39	0.30
1 : 5	0.60	1.29	0.42	0.32
1 : 6	0.57	0.88	0.37	0.18
DSi-6T : PCBM (with TiO_2)				
1 : 4	0.64	1.34	0.50	0.42
1 : 5	0.60	1.34	0.55	0.44
1 : 6	0.62	1.07	0.49	0.32
DH-6T : PCBM				
1 : 4	0.52	0.62	0.33	0.11
1 : 6	0.63	0.60	0.44	0.17
DH-6T : PCBM (with TiO_2)				
1 : 4	0.51	0.61	0.42	0.13
1 : 6	0.65	0.57	0.56	0.21

[a]Open circuit voltage (V_{oc}), short circuit current density (J_{sc}), fill factor (FF), and PCE at DSi-6T and DH-6T as electron donors: PCBM at weight ratio. The device performance was consistent and reproducible. The active area is 0.12 cm^2.

the TiO_2 interfacial layer improved the PCEs and reduced the sensitivity of such devices to oxygen and water vapour [21, 28]. As shown in Figure 4, the FF of **DSi-6T** : PCBM cells with TiO_2 layer is enhanced up to 0.55 which is 30% higher than that of the solar cell. The best performance was observed on **DSi-6T** : PCBM 1 : 5 (w/w) blend cell with V_{oc} of 0.63 V, J_{sc} of 1.34 mA/cm^2, FF of 55%, and power conversion efficiency of 0.44%. Also the FF of **DH-6T** cells is exactly 27% higher than that of solar cells. The **DH-6T** : PCBM 1 : 6 (w/w) blend cell with TiO_2 layer exhibited a V_{oc} of 0.65 V, J_{sc} of 0.57 mA/cm^2, FF of 56%, and PCE of 0.21% (Figure 5). The incorporation of solution processed TiO_2 interfacial layer in the sexithiophene : PCBM BHJ devices significantly enhances FF, mainly due to the reduced charge recombination near active layer/Al interface.

Figure 6 shows the external quantum efficiency (EQE) plot for the **DSi-6T** : PCBM (1 : 5 w/w) and **DH-6T** : PCBM (1 : 6 w/w) cells. The sexithiophene-based cells absorb the solar light in narrow visible range and show low EQEs due to a small amount of donor by limited solubility. For the **DH-6T** : PCBM solar cell, the maximum EQE is 11.3% at 340 nm that is caused by strong absorption of PCBM. When the **DSi-6T** was used, the **DSi-6T** : PCBM solar cell shows a higher EQE in the all wavelength, with a maximum of 16.1% at 410 nm. The absorption of the **DSi-6T** donor was increased in the EQE spectrum to be different from the UV-vis spectrum. It is expected that horizontal intermolecular packing due to the bulky silyl side chains of **DSi-6T** may increase the charge transfer at the interfaces, so the EQE increases.

To investigate the charge transporting property of the OPV devices, we measured hole mobility of the donor: PCBM blend layers with the space-charge limited-current (SCLC) model. Hole-only devices were fabricated with a device configuration of ITO/PEDOT : PSS/Donor : PCBM/MoO_3/Al, because high work function of molybdenum oxide (MoO_3) blocks the injection of electrons from the Al cathode. The blend ratios of the Donor: PCBM layers were 1 : 5 (w/w) and 1 : 6 (w/w) for **DSi-6T** : PCBM and **DH-6T** : PCBM, respectively.

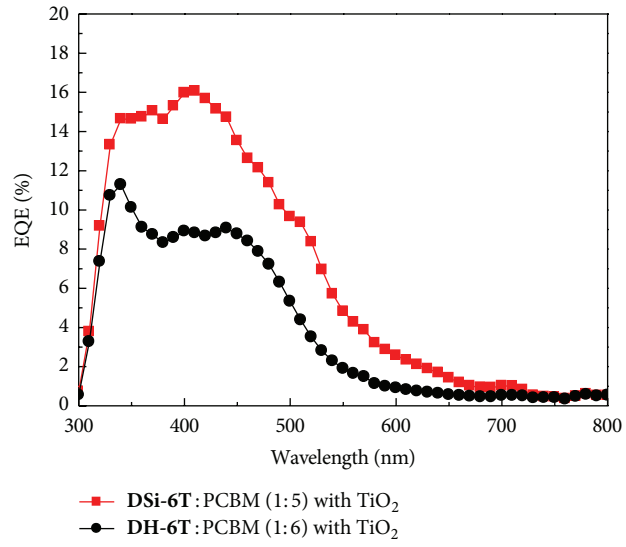

Figure 6: EQE curves of **DSi-6T** : PCBM (1 : 5) and **DH-6T** : PCBM (1 : 6) blend cells.

The hole transport through the active layers is limited by the space charge and the SCLC is described by

$$J = \frac{9}{8}\varepsilon_r \varepsilon_0 \mu_h \frac{V^2}{L^3}, \quad (2)$$

where J is the current density, ε_0 is the permittivity of vacuum, ε_r is the dielectric constant of the material (assumed to be 3), μ_h is the mobility, V is the applied voltage ($V_{applied}$) corrected from built-in voltage (V_{bi}) arising from difference in the work function of the contacts and voltage drop (V_r) due to the series resistance of the electrodes, and L is the thickness of the blend layer [29]. Equation (1) is valid when the mobility

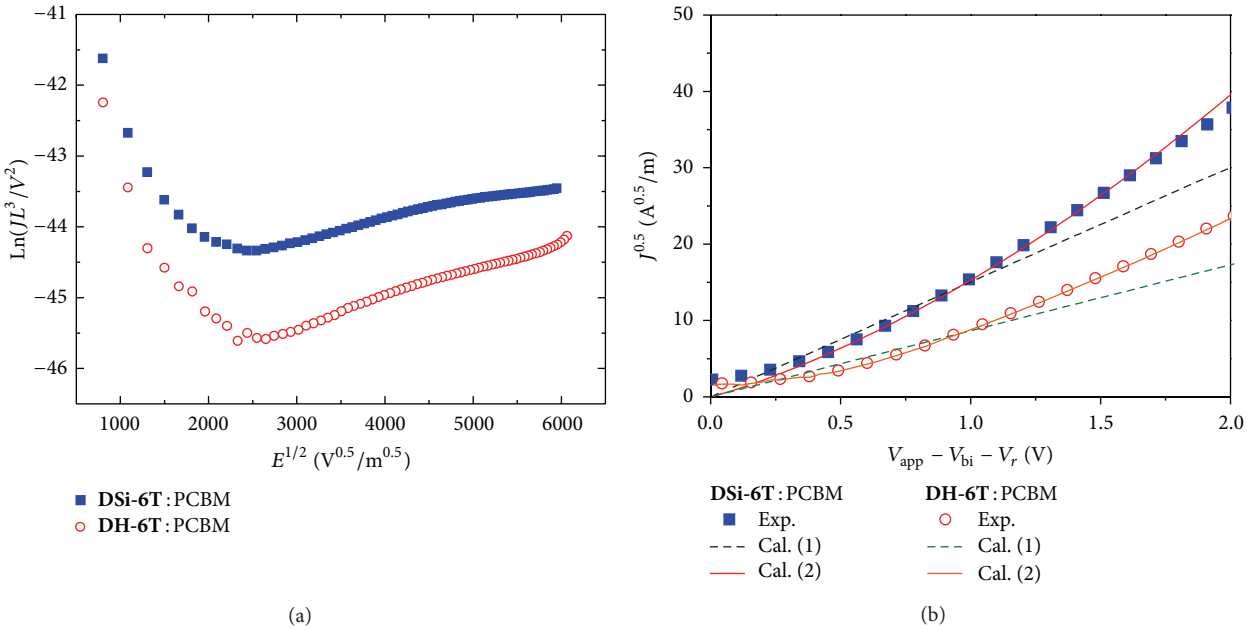

FIGURE 7: (a) $\ln(JL^3/V^2)$ versus $E^{1/2}$ curves according to the SCLC equation (2). (b) $J^{1/2}$ versus V curves showing the electric-field-dependence of hole mobilities at highly biased region. Dotted and solid lines are calculated curves with (1) and (2), respectively.

is field independent. It has been found that the behaviour of electric field dependence of the mobility can be described by an empirical rule; $\mu_h = \mu_{h0} \exp(\gamma E^{1/2})$, where μ_{h0} is the hole mobility at zero field, γ is field dependence prefactor, and E is the electric field. Therefore, the electric field dependent SCLC model can be expressed by

$$J = \frac{9}{8}\varepsilon_r \varepsilon_0 \mu_{h0} \exp\left(\gamma\sqrt{E}\right)\frac{V^2}{L^3}. \quad (3)$$

The zero-field hole mobility μ_{h0} and the prefatory γ of **DSi-6T** : PCBM (1 : 5 w/w) and **DH-6T** : PCBM (1 : 6 w/w) blend films were obtained from (2) as shown in Figure 7(a) ($\mu_{h0} = 7.7 \times 10^{-6}\,\text{cm}^2/\text{Vs}$, $\gamma = 3.3 \times 10^{-4}\,\text{m}^{0.5}\,\text{V}^{-0.5}$ for **DSi-6T** : PCBM, and $\mu_{h0} = 1.6 \times 10^{-6}\,\text{cm}^2/\text{Vs}$, $\gamma = 4.5 \times 10^{-4}\,\text{m}^{0.5}\,\text{V}^{-0.5}$ for **DH-6T** : PCBM). The low γ of **DSi-6T** : PCBM indicates low energetic disorder related to the interaction of each hopping charge in randomly oriented dipoles [30, 31]. Figure 7(b) shows the SCLC fitting of **DSi-6T** : PCBM (1 : 5 w/w) and **DH-6T** : PCBM (1 : 6 w/w) blend films according to (1) and (2). It is observed that the SCLC calculated from the field independent model deviates from the experimental data at the high voltage region. In actual operating devices, the active materials are in the effective bias of ~1 V (corresponding to the energy level difference of HOMO and LUMO of an electron donor and acceptor) at the short circuit conditions. Taking this into consideration, we estimated the field dependent hole mobility of the active blend layers at 1 V; $\mu_h = 2.7 \times 10^{-5}\,\text{cm}^2/\text{Vs}$ for **DSi-6T** : PCBM, and $\mu_h = 8.8 \times 10^{-6}\,\text{cm}^2/\text{Vs}$ for **DH-6T** : PCBM. The higher hole mobility of the **DSi-6T** : PCBM blend film than that of the **DH-6T** : PCBM film is a key property of the enhanced photovoltaic performance. It seems that the higher hole mobility of **DSi-6T** : PCBM blend layer is inconsistent with the pure donor's field-effect mobility. However, it should be noted that the mobility in organic thin-film transistors strongly depends on the molecular orientation due to the highly anisotropic charge carrier mobility. In the OPV device configuration, the **DSi-6T** : PCBM BHJ layer yielded the better vertical charge transport than the **DH-6T** : PCBM due to the improved solubility of **DSi-6T**.

To study the thermal annealing effect of this system, the morphologies of sexithiophene: PCBM films before and after annealing at 60°C were studied by atomic force microscopy (AFM) (Figure 8). The morphological studies indicate the more amorphous nature of **DSi-6T** : PCBM compared to **DH-6T** : PCBM films. The root-mean-square (rms) roughness is 47, 38, and 23 nm for **DSi-6T** : PCBM 1 : 4, 1 : 5, and 1 : 6 (w/w), respectively, and 7.1 nm for **DH-6T** : PCBM 1 : 6 (w/w). In **DSi-6T** : PCBM films, the weight ratio donor to acceptor increased as the roughness of films decreased. After thermal annealing, the roughness was 37, 29, and 14 nm for **DSi-6T** : PCBM 1 : 4, 1 : 5, 1 : 6 (w/w), respectively, and 7.6 nm for **DH-6T** : PCBM 1 : 6 (w/w). For the solar cell based on the **DSi-6T** : PCBM cell, the rms roughness of films after thermal annealing at 60°C was significantly reduced as compared to that of films. In the case of **DH-6T** : PCBM cell, the morphological change after annealing was slightly observed. Unfortunately, all films were quite rough compared to the polymer solar cells. The inferior morphologies of sexithiophene based BHJ solar cells may be related to the solubility of donors, which is expected to influence the photovoltaic performance. For a comparison, the **DSi-6T** : PCBM cell was thermally annealed at 135°C which was the temperature employed for the P3HT : PCBM cell. When a film was annealed at a high temperature, the decrease in

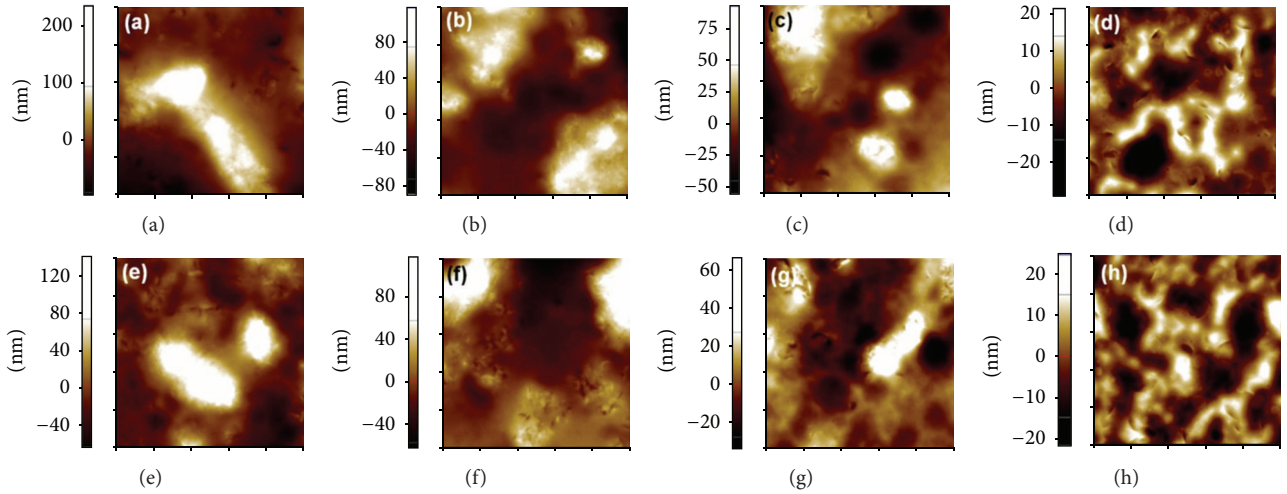

Figure 8: AFM images of the blended films under various ratios (a) **DSi-6T** : PCBM 1 : 4 w/w nonannealed (e) annealed and (b) **DSi-6T** : PCBM 1 : 5 w/w non-annealed (f) annealed and (c) **DSi-6T** : PCBM 1 : 6 w/w non-annealed (g) annealed and (d) **DH-6T** : PCBM 1 : 6 w/w non-annealed (h) annealed. The image scan sizes is 5 μm × 5 μm.

PCE (0.034%) became more significant. The future work may concentrate on optimization of the annealing temperature of the **DSi-6T** : PCBM devices to allow better efficiency.

4. Conclusion

In conclusion, we have demonstrated solution processed organic photovoltaic cells that incorporate sexithiophene derivatives having silyl side chain or hexyl chain in the end of thiophene ring as donor materials and PCBM as an acceptor. Owing to the particular electronic properties of **DSi-6T**, **DH-6T**, and PCBM, such combinations seem to be perfectly suited for the study of electron-transfer processes in the polar media via the triplet states. The electron-transfer process from the triplet states of **DSi-6T**, **DH-6T** to PCBM was confirmed in this study by utilizing the nanosecond laser photolysis technique in the visible and NIR regions. **DSi-6T** showed higher photovoltaic performance than **DH-6T**, despite its poor quality film morphology. The optimal **DSi-6T** : PCBM blend ratio was found to be 1 : 5, and its power conversion efficiency was 0.44% under AM 1.5 G illumination. Although the power conversion efficiency remains to be improved, the present study provides valuable insight into the further development of the solution-processed efficient OPV devices.

Conflict of Interests

The authors declare that they have no conflict of interests.

Acknowledgments

This research was supported by Grants-in-Aid (No. 20108010) from the Ministry of Education, Culture, Sports, Science and Technology, Japan, and NRF/MEST of Korea through WCU (R31-2008-000-10010-0) and GRL (2010-00353) Programs.

References

[1] G. Yu, J. Gao, J. C. Hummelen, F. Wudl, and A. J. Heeger, "Polymer photovoltaic cells: enhanced efficiencies via a network of internal donor-acceptor heterojunctions," *Science*, vol. 270, no. 5243, pp. 1789–1791, 1995.

[2] N. S. Sariciftci, L. Smilowitz, A. J. Heeger, and F. Wudl, "Photoinduced electron transfer from a conducting polymer to buckminsterfullerene," *Science*, vol. 258, no. 5087, pp. 1474–1476, 1992.

[3] S. Günes, H. Neugebauer, and N. S. Sariciftci, "Conjugated polymer-based organic solar cells," *Chemical Reviews*, vol. 107, no. 4, pp. 1324–1338, 2007.

[4] P. W. M. Blom, V. D. Mihailetchi, L. J. A. Koster, and D. E. Markov, "Device physics of polymer: fullerene bulk heterojunction solar cells," *Advanced Materials*, vol. 19, no. 12, pp. 1551–1566, 2007.

[5] W. Tang, J. Hai, Y. Dai et al., "Recent development of conjugated oligomers for high-efficiency bulk-heterojunction solar cells," *Solar Energy Materials and Solar Cells*, vol. 94, no. 12, pp. 1963–1979, 2010.

[6] H.-Y. Chen, J. Hou, S. Zhang et al., "Polymer solar cells with enhanced open-circuit voltage and efficiency," *Nature Photonics*, vol. 3, no. 11, pp. 649–653, 2009.

[7] Y. Liang, Z. Xu, J. Xia et al., "For the bright future-bulk heterojunction polymer solar cells with power conversion efficiency of 7.4%," *Advanced Materials*, vol. 22, no. 20, pp. E135–E138, 2010.

[8] *Electronic Materials: The Oligomer Approach*, edited by K. Müllen and G. Wegner, Wiley-VCH, Weinheim, Germany, 1998.

[9] *Handbook of Oligo- and Polythiophenes*, edited by D. Fichou, Wiley-VCH, Weinheim, Germany, 1999.

[10] A. Mishra, C.-Q. Ma, and P. Bäuerle, "Functional oligothiophenes: molecular design for multidimensional nanoarchitectures and their applications," *Chemical Reviews*, vol. 109, no. 3, pp. 1141–1176, 2009.

[11] N. Noma, T. Tsuzuki, and Y. Shirota, "α-thiophene octamer as a new class of photoactive material for photoelectrical conversion," *Advanced Materials*, vol. 7, no. 7, pp. 647–648, 1995.

[12] C. Videlot, A. El Kassmi, and D. Fichou, "Photovoltaic properties of octithiophene-based Schottky and p/n junction cells: influence of molecular orientation," *Solar Energy Materials and Solar Cells*, vol. 63, no. 1, pp. 69–82, 2000.

[13] P. Liu, Q. Li, M. Huang, W. Pan, and W. Deng, "High open circuit voltage organic photovoltaic cells based on oligothiophene derivatives," *Applied Physics Letters*, vol. 89, no. 21, pp. 213501–213503, 2006.

[14] K. Schulze, C. Uhrich, R. Schüppel et al., "Efficient vacuum-deposited organic solar cells based on a new low-bandgap oligothiophene and fullerene C_{60}," *Advanced Materials*, vol. 18, no. 21, pp. 2872–2875, 2006.

[15] J. Ah Kong, E. Lim, K. K. Lee, S. Lee, and S. Hyun Kim, "A benzothiadiazole-based oligothiophene for vacuum-deposited organic photovoltaic cells," *Solar Energy Materials and Solar Cells*, vol. 94, no. 12, pp. 2057–2063, 2010.

[16] J. Sakai, T. Taima, and K. Saito, "Efficient oligothiophene:fullerene bulk heterojunction organic photovoltaic cells," *Organic Electronics*, vol. 9, no. 5, pp. 582–590, 2008.

[17] M. Halik, H. Klauk, U. Zschieschang et al., "Relationship between molecular structure and electrical performance of oligothiophene organic thin film transistors," *Advanced Materials*, vol. 15, no. 11, pp. 917–922, 2003.

[18] J. H. Choi, D. W. Cho, H. J. Park et al., "Synthesis and characterization of a series of bis(dimethyl-n-octylsilyl)oligothiophenes for organic thin film transistor applications," *Synthetic Metals*, vol. 159, no. 15-16, pp. 1589–1596, 2009.

[19] F. Garnier, A. Yassar, R. Hajlaoui et al., "Molecular engineering of organic semiconductors: design of self-assembly properties in conjugated thiophene oligomers," *Journal of the American Chemical Society*, vol. 115, no. 19, pp. 8716–8721, 1993.

[20] E. Scolan and C. Sanchez, "Synthesis and characterization of surface-protected nanocrystalline titania particles," *Chemistry of Materials*, vol. 10, no. 10, pp. 3217–3223, 1998.

[21] W.-S. Chung, H. Lee, W. Lee et al., "Solution processed polymer tandem cell utilizing organic layer coated nano-crystalline TiO_2 as interlayer," *Organic Electronics*, vol. 11, no. 4, pp. 521–528, 2010.

[22] A. Sassella, R. Tubino, A. Borghesi et al., "Optical properties of oriented thin films of oligothiophenes," *Synthetic Metals*, vol. 101, no. 1, pp. 538–541, 1999.

[23] S. Cook, H. Ohkita, Y. Kim, J. J. Benson-Smith, D. D. C. Bradley, and J. R. Durrant, "A photophysical study of PCBM thin films," *Chemical Physics Letters*, vol. 445, no. 4-6, pp. 276–280, 2007.

[24] D. Rehm and A. Weller, "Kinetik und mechanismus der elektronübertragung bei der fluoreszenzlöschung in acetonitril," *Berichte der Bunsengesellschaft für physikalische Chemie*, vol. 73, pp. 834–839, 1969.

[25] R. J. Sension, A. Z. Szarka, G. R. Smith, and R. M. Hochstrasser, "Ultrafast photoinduced electron transfer to C_{60}," *Chemical Physics Letters*, vol. 185, no. 3-4, pp. 179–183, 1991.

[26] *Handbook of Photochemistry*, edited by S. I. Murov, Marcel Dekker, New York, NY, USA, 1985.

[27] M. E. El-Khouly, O. Ito, P. M. Smith, and F. D'Souza, "Intermolecular and supramolecular photoinduced electron transfer processes of fullerene-porphyrin/phthalocyanine systems," *Journal of Photochemistry and Photobiology C*, vol. 5, no. 1, pp. 79–104, 2004.

[28] K. Lee, J. Y. Kim, S. H. Park, S. H. Kim, S. Cho, and A. J. Heeger, "Air-stable polymer electronic devices," *Advanced Materials*, vol. 19, no. 18, pp. 2445–2449, 2007.

[29] P. W. M. Blom, M. J. M. de Jong, and M. G. van Munster, "Electric-field and temperature dependence of the hole mobility in poly(p-phenylene vinylene)," *Physical Review B*, vol. 55, no. 2, pp. R656–R659, 1997.

[30] D. H. Dunlap, P. E. Parris, and V. M. Kenkre, "Charge-dipole model for the universal field dependence of mobilities in molecularly doped polymers," *Physical Review Letters*, vol. 77, no. 3, pp. 542–545, 1996.

[31] G. G. Malliaras, J. R. Salem, P. J. Brock, and C. Scott, "Electrical characteristics and efficiency of single-layer organic light-emitting diodes," *Physical Review B*, vol. 58, no. 20, pp. R13411–R13414, 1998.

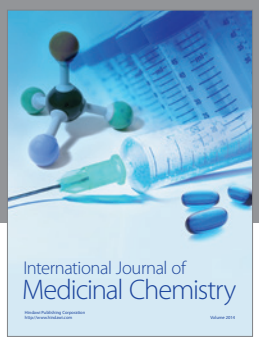

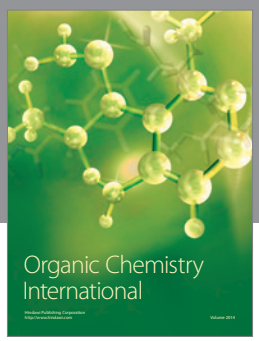

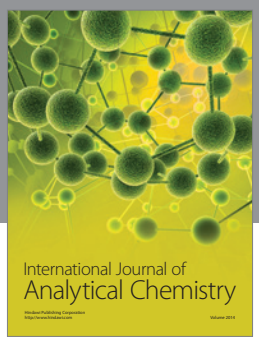

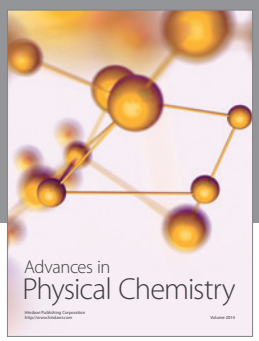

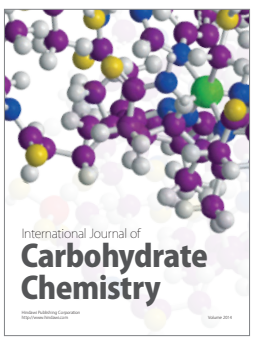

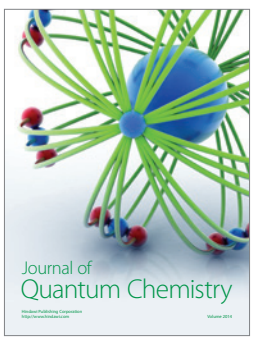

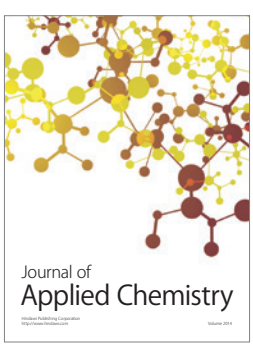

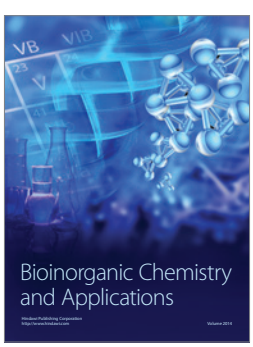

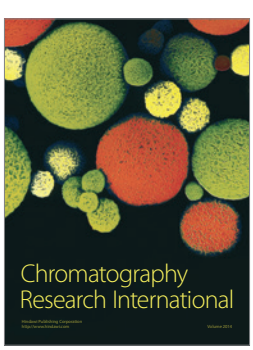

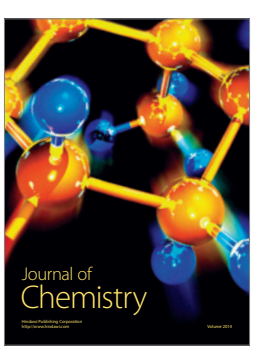

Hindawi

Submit your manuscripts at
http://www.hindawi.com